

Coordinated path following control of multi-unicycle formation motion around closed curves in a time-invariant flow

Yang-Yang Chen · Yu-Ping Tian

Received: 10 April 2014 / Accepted: 19 March 2015 / Published online: 8 April 2015
© Springer Science+Business Media Dordrecht 2015

Abstract This paper utilizes a dynamic model of unicycles to address the stabilization of formation motion around closed curves in the presence of a time-invariant flow field. It is shown that our previous concentric compression design can be extended to deal with robust coordinated path following control for fighting against the external flow field. Linear acceleration control for each unicycle is used and combined with the rotation control to achieve both temporal and spatial formations in the case of a spatially variable flow, which breaks the restriction of temporally balanced formation relied solely on the angle control in the literature. A potential function is introduced to force each unicycle's speed greater than the magnitude of flow. The theoretical result is proved by two numerical examples.

Keywords Robust coordinated path following control · Unicycles · Curve extension · Nonlinear dynamics

1 Introduction

Recent advances in control techniques for autonomous vehicles and agile sensor networks bring researchers the dawn to apply a family of sensor-equipped vehicles to execute surveillance [1], environmental fields measurement [2,3] and persistent survey of biological system [4]. In almost any environment, the sensory performance has been severely affected by an external flow field (e.g., ocean current or atmospheric wind). For example, the atmospheric wind can push each unicycle away from its given path and disrupt the relative position of each pair of unicycles (that is formation), which leads to reducing the accuracy of data sampling. Nowadays, most existing coordinated path following control protocols [5–13] are derived based on flow-free motion models, and thus, they often fail to account for the degradation of control performance caused by flow fields. Therefore, it is urgently needed to design a robust coordinated path following control when vehicles suffer an external flow field.

Although robust consensus control with disturbances of the external environment are well discussed in the literature [14–16], prior works on robust coordinated path following control for fighting against an external flow field are still few due to the geometric constraints on the vehicles' movements (that is, each vehicle must follow its given orbit). In [17], an angular velocity algorithm is provided for each constant-speed particle to stabilize the temporally balanced formation around a circle in a steady, uniform flow field and then

Y.-Y. Chen · Y.-P. Tian
School of Automation, Southeast University,
Nanjing 210096, People's Republic of China

Y.-Y. Chen (✉) · Y.-P. Tian
Key Laboratory of Measurement and Control of Complex
Systems of Engineering, Ministry of Education, Southeast
University, Nanjing 210096, People's Republic of China
e-mail: yychen@seu.edu.cn

Y.-P. Tian
e-mail: yptian@seu.edu.cn

extended to deal with double integrators by the backstepping technology [18]. A similar idea is used to give a solution to coordinate UAVs flying around a convex loop in a spatially invariant wind [19]. Furthermore, all the above results [17–19] are based on the assumption that the magnitude of the flow is weaker than the vehicle's speed. It must be emphasized that one relying solely on the angle control cannot maintain the spatial formation (that is the uniform separation around orbits) even in the simplest case of a steady, uniform flow field. This is due to the fact that the external flow leads to the various actual linear speed of the vehicle at different locations even though the vehicle satisfies constant speed. Since the exact spatial formation is important to the accuracy of data measurements and the (near) optimal sampling trajectory for each vehicle is often planned to be a simple and closed curve (not limited in a circle or a convex loop) [2–4], we discuss coordinated path following control for the temporal and spatial formation motions around a set of closed orbits in an external flow field.

This paper builds upon our prior research on the geometric extension design. The key idea of this approach is to extend the given curve to be a set of level curves of the orbit function for path following and then incorporate the orbit function into the arc-length function to give the solution to formation motion around the given orbits. In the absence of a flow field, coordinated Newtonian particle formation motion around closed curves is solved based on the geometric extension along each curve's normal vector [9, 10]. To maintain the same geometric topology among the extended curves and the given curve, Chen and Tian propose the concentric compression design to deal with cooperative motion along convex loops at first [11, 12] and then a kind of general non-convex and closed curves [13]. However, the result of using the geometric extension design for coordinated path following control in the presence of a time-invariant flow field is not established yet.

The main contribution of this paper is that we show that the concentric compression design can be extended to deal with the temporal and spatial formation motions around a family of given closed curves in the presence of a flow field, which breaks the restriction of temporally balanced formation on a circle or a convex loop when vehicles suffer an external flow in the literature [17–19]. The external flow field under consideration is known, non-uniform and time-invariant, which covers the types of the flow field discussed in [17–19]. We

deal with the control of the unicycle's dynamics which is the difference from the constant-speed particle on the additional linear acceleration control. In this paper, the inertial velocity of the flow is first converted to the linear speed and the orientation of the unicycle. Then, the component where the linear acceleration and the angular acceleration are projected onto the actual orientation of each unicycle is used to accomplish both temporal and spatial formations, and at the same time, the component where the linear acceleration and the angular acceleration are projected onto the normal vector perpendicular to the actual orientation of each unicycle is applied to achieve the orbit tracking. For the purpose of ensuring that each unicycle's speed is greater than the magnitude of flow, a potential function often used in collision avoidance [21] is introduced into the controller design.

This paper is organized as follows. Section 2 summarizes the unicycle's model in an external flow field and formulates the coordinated control problem based on concentric compression. In Sect. 3, the control design scheme is designed based on the backstepping technology. Simulation results are given in Sect. 4. Section 5 provides conclusion.

2 Problem statement

2.1 Unicycle's model in a time-invariant flow field

In this subsection, we will show the dynamic model of a unicycle in a time-invariant flow field. Each unicycle is subject to two independent control inputs $\{u_i, \tau_i\}$ in order to provide the linear acceleration force and the angular moment in the flow field. Let $\mathbf{z}_i = [z_i^x, z_i^y]^T \in \mathbb{R}^2$ indicate the position of the wheel axis center defined in an inertia coordinate frame \mathcal{W} . Also let θ_i be the i th unicycle's orientation with respect to the x -axis of \mathcal{W} . v_i and ω_i are its linear and angular velocities, respectively. In this paper, the flow field is known and time-invariant. Its inertial velocity at \mathbf{z}_i is represented as $\mathbf{f}(\mathbf{z}_i) = [f^x(\mathbf{z}_i), f^y(\mathbf{z}_i)]^T$ such that $\|\mathbf{f}\| \leq f_M$ where f_M is a bounded constant. With loss of generality, the flow field is permitted to be spatially variable (non-uniform) as long as it is C^2 smooth where $\mathbf{f}' = \partial \mathbf{f} / \partial \mathbf{z}_i = [\nabla f^x, \nabla f^y]^T = \begin{bmatrix} \partial f^x / \partial z_i^x & \partial f^x / \partial z_i^y \\ \partial f^y / \partial z_i^x & \partial f^y / \partial z_i^y \end{bmatrix}$. The dynamics of a unicycle in the presence of a time-invariant flow field (see Fig. 1) is

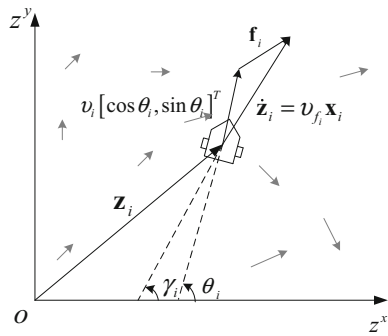


Fig. 1 Unicycle’s model in a time-invariant flow field

$$\begin{cases} \dot{z}_i^x = v_i \cos \theta_i + f^x \\ \dot{z}_i^y = v_i \sin \theta_i + f^y \\ \dot{\theta}_i = \omega_i \\ \dot{v}_i = u_i \\ \dot{\omega}_i = \tau_i \end{cases} \quad (1)$$

Remark 1 In [18, 19], only a uniform, time-invariant flow so that $\mathbf{f} = [\beta, 0]^T$ is considered where constant β satisfies that $|\beta| < 1$ due to the unit speed of each particle. A simple non-uniform time-invariant flow $\mathbf{f} = [f^x(z_i^x), f^y(z_i^y)]^T$ is discussed in [17]. Compared with the flow field considered in this paper, each above-mentioned flow field can be regarded as a special case of this paper.

Let $\gamma_i = \arctan 2(\dot{z}_i^x, \dot{z}_i^y)$ be the orientation of the actual inertial velocity of the i th unicycle and $v_{f_i} = \|\dot{\mathbf{z}}_i + \mathbf{f}\|$ denote its magnitude. Also let $\mathbf{x}_i = [\cos \gamma_i, \sin \gamma_i]^T$ be the unit vector tangent to the trajectory of the i th unicycle at the current location and the normal vector \mathbf{y}_i is perpendicular to \mathbf{x}_i . The dynamics of the position of the i th unicycle can be written as $\dot{\mathbf{z}}_i = v_{f_i} \mathbf{x}_i$. In the following, we first show the dynamics of γ_i . From the first two equations of (1), we have

$$\tan \gamma_i = \frac{v_i \sin \theta_i + f^y}{v_i \cos \theta_i + f^x}. \quad (2)$$

Differentiating (2) with respect to time along the solution of (1) for $\dot{\gamma}_i$, we obtain

$$\dot{\gamma}_i = \kappa_{\gamma_i}^u u_i + \kappa_{\gamma_i}^\omega \omega_i + d_{\gamma_i} \quad (3)$$

where

$$\begin{aligned} \kappa_{\gamma_i}^u &= -v_i^{-1} v_{f_i}^{-1} f_i^y \cos \gamma_i + v_i^{-1} v_{f_i}^{-1} f_i^x \sin \gamma_i \\ &= -v_i^{-1} v_{f_i}^{-1} (\mathbf{f}_i \cdot \mathbf{y}_i), \end{aligned}$$

$$\begin{aligned} \kappa_{\gamma_i}^\omega &= 1 - v_{f_i}^{-1} (f_i^x \cos \gamma_i + f_i^y \sin \gamma_i) \\ &= 1 - v_{f_i}^{-1} (\mathbf{f}_i \cdot \mathbf{x}_i), \\ d_{\gamma_i} &= (\nabla f^x \cdot \mathbf{x}_i) \cos \gamma_i - (\nabla f^y \cdot \mathbf{x}_i) \sin \gamma_i. \end{aligned}$$

It is obvious that Eq. (3) is suitable when $v_i > \|\mathbf{f}\|$ or $v_i < \|\mathbf{f}\|$. In this paper, we only consider the situation that $v_i > \|\mathbf{f}\|$. Next we will express v_{f_i} as a function of $(v_i, \mathbf{f}, \gamma_i)$. Also from the first two equations of (1), one gets

$$v_{f_i} = \sqrt{v_i^2 - \|\mathbf{f}\|^2 + 2(\mathbf{f} \cdot \mathbf{x}_i) v_{f_i}} \quad (4)$$

which implies

$$v_{f_i}^2 - 2(\mathbf{f} \cdot \mathbf{x}_i) v_{f_i} + \|\mathbf{f}\|^2 - v_i^2 = 0. \quad (5)$$

When $v_i > \|\mathbf{f}\|$, the quadratic Eq. (5) has the solution

$$v_{f_i} = \mathbf{f} \cdot \mathbf{x}_i + \sqrt{v_i^2 - (\mathbf{f} \cdot \mathbf{y}_i)^2}. \quad (6)$$

Differentiating (6) with respect to time along the solution of (1) and solving for \dot{v}_{f_i} using (3), we obtain

$$\dot{v}_{f_i} = \kappa_{v_{f_i}}^u u_i + \kappa_{v_{f_i}}^\omega \omega_i + d_{v_{f_i}} \quad (7)$$

where

$$\begin{aligned} \kappa_{v_{f_i}}^u &= \kappa_{\gamma_i}^u \left[(\mathbf{f}_i \cdot \mathbf{y}_i) - (v_i^2 - (\mathbf{f}_i \cdot \mathbf{y}_i)^2)^{-\frac{1}{2}} \right. \\ &\quad \times (\mathbf{f}_i \cdot \mathbf{y}_i) (\mathbf{f}_i \cdot \mathbf{x}_i) \left. \right] \\ &\quad + (v_i^2 - (\mathbf{f}_i \cdot \mathbf{y}_i)^2)^{-\frac{1}{2}} v_i, \\ \kappa_{v_{f_i}}^\omega &= \kappa_{\gamma_i}^\omega \left[(\mathbf{f} \cdot \mathbf{y}_i) - (v_{f_i} - \mathbf{f} \cdot \mathbf{x}_i)^{-1} (\mathbf{f} \cdot \mathbf{y}_i) (\mathbf{f} \cdot \mathbf{x}_i) \right], \\ d_{v_{f_i}} &= v_{f_i} (\mathbf{f}' \mathbf{x}_i) \cdot \mathbf{x}_i \\ &\quad - v_{f_i} (v_{f_i} - \mathbf{f} \cdot \mathbf{x}_i)^{-1} (\mathbf{f} \cdot \mathbf{y}_i) (\mathbf{f}' \mathbf{x}_i) \cdot \mathbf{y}_i. \end{aligned}$$

Furthermore, one gets $v_i = \sqrt{v_{f_i}^2 - 2(\mathbf{f} \cdot \mathbf{x}_i) v_{f_i} + \|\mathbf{f}\|^2}$ from (5) and then $\kappa_{\gamma_i}^u$ can be rewritten as

$$\kappa_{\gamma_i}^u = v_{f_i}^{-1} (v_{f_i}^2 - 2(\mathbf{f} \cdot \mathbf{x}_i) v_{f_i} + \|\mathbf{f}\|^2)^{-\frac{1}{2}} (\mathbf{f} \cdot \mathbf{y}_i).$$

In the Sect. 3, we first regard ω_i as a virtual control and then apply the backstepping technology to design τ_i . By using (3) and (7) to calculate (ω_i, u_i) , it is required

$$\begin{vmatrix} \kappa_{\gamma_i}^u & \kappa_{\gamma_i}^\omega \\ \kappa_{v_{f_i}}^u & \kappa_{v_{f_i}}^\omega \end{vmatrix} \neq 0 \quad (8)$$

which implies

$$\begin{aligned} g_{\kappa_i} &= \sqrt{v_{f_i}^2 - 2(\mathbf{f} \cdot \mathbf{x}_i) v_{f_i} + \|\mathbf{f}\|^2} (v_{f_i} - \mathbf{f} \cdot \mathbf{x}_i)^{-1} \\ &\quad \times (1 - v_{f_i}^{-1} (\mathbf{f} \cdot \mathbf{x}_i)) \neq 0. \end{aligned} \quad (9)$$

(9) is true when $v_i > \|\mathbf{f}\|$ and the proof is similar to the procedure described in [17].

From the above discussion, the dynamics of unicycle with a time-invariant flow becomes

$$\begin{cases} \dot{\mathbf{z}}_i = v_{f_i} \mathbf{x}_i \\ \dot{\mathbf{x}}_i = (\kappa_{\gamma_i}^u u_i + \kappa_{\gamma_i}^\omega \omega_i + d_{\gamma_i}) \mathbf{y}_i \\ \dot{\mathbf{y}}_i = -(\kappa_{\gamma_i}^u u_i + \kappa_{\gamma_i}^\omega \omega_i + d_{\gamma_i}) \mathbf{x}_i \\ \dot{v}_{f_i} = \kappa_{v_{f_i}}^u u_i + \kappa_{v_{f_i}}^\omega \omega_i + d_{v_{f_i}} \\ \dot{\omega}_i = \tau_i \end{cases} \quad (10)$$

Remark 2 As compared with the model of unit-speed particle in a time-invariant flow field [17–19], the dynamic model (10) with the acceleration control is more complex. $\kappa_{v_{f_i}}^u u_i + \kappa_{v_{f_i}}^\omega \omega_i$ is the term where the linear acceleration and the angular acceleration are projected onto \mathbf{x}_i , and we use it to accomplish the temporal and spatial formations. $\kappa_{\gamma_i}^u u_i + \kappa_{\gamma_i}^\omega \omega_i$ is the component where the linear acceleration and the angular acceleration are projected onto \mathbf{y}_i , and it is used to achieve the orbit tracking. In Subsect. 3.2, these two components are designed at first and then used to solve u_i and ω_i . At last, τ_i is obtained by using the backstepping technology.

2.2 Concentric-compressing-based design

Consider that the given orbit Γ_{i0} associated with the i th unicycle is a simple and closed curve with nonzero curvature. Suppose that Γ_{i0} can be parameterized by using a smooth map $\Gamma_{i0} : [0, 2\pi) \rightarrow \mathbb{R}^2, \phi_i \mapsto \Gamma_{i0}(\phi_i)$ with $\|\Gamma_{i0}(\phi_i)\| > 0$ and $\|d\Gamma_{i0}(\phi_i)/d\phi_i\| > 0$, where ϕ_i is the phase angle that describes the direction of the vector from the origin of the orbit to the point on the orbit with respect to the positive axis of \mathcal{W} . Also assume that the vector from the origin of the orbit to each point $\mathbf{z}_{i,k}$ on the orbit and the tangent vector to the orbit on $\mathbf{z}_{i,k}$ are linearly independent, that is $\left| \Gamma_{i0}(\phi_i), \frac{d\Gamma_{i0}(\phi_i)}{d\phi_i} \right| \neq 0$ for all ϕ_i . Referring to Lemma 1 in [13], a set of orbits can be obtained by concentric compressing, that is

$$\Gamma_{i\lambda}(\phi_i, \lambda) = (1 - \lambda) \Gamma_{i0}(\phi_i) \quad (11)$$

and each one corresponds to a special constant value of the orbit function $\lambda_i(\mathbf{z}_i)$, where $\lambda_i(\mathbf{z}_i)$ satisfies $\nabla \lambda_i(\mathbf{z}_i) \neq 0$ and $|\lambda_i(\mathbf{z}_i)| < \varepsilon_i, (\varepsilon_i > 0)$. The orbit value associated with the given orbit Γ_{i0} is 0 (see Fig. 2). Some corresponding proofs and examples can be found in [11, 13].

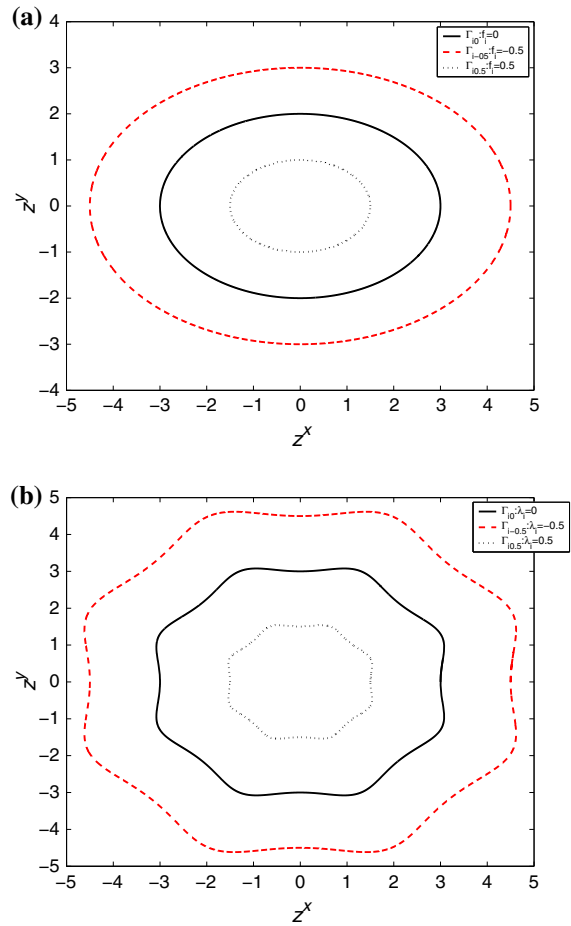


Fig. 2 Concentric compression: **a** A family of convex and closed curves, **b** A family of non-convex and closed curves

In order to follow the given orbit, the path following control should drive the orbit value $\lambda_i(\mathbf{z}_i)$ and the direction error $\alpha_i \in (-\pi, \pi]$ between the unicycle’s motion and the tangent vector to the orbit to 0 asymptotically (see Fig. 3), i.e.,

$$\lim_{t \rightarrow \infty} \lambda_i(\mathbf{z}_i(t)) = 0, \quad (12)$$

$$\lim_{t \rightarrow \infty} \alpha_i(t) = 0, \quad (13)$$

Due to the domain of the orbit function, the trajectory of each unicycle should be limited in the set Ω_i , i.e.,

$$|\lambda_i(\mathbf{z}_i(t))| < \varepsilon_i. \quad (14)$$

When each unicycle moves along its given orbit, the control object is to achieve the desired formation with the given orbits adopted. To this end, communication among the unicycles is essential. Let $\mathcal{G} = \{\mathcal{V}, \mathcal{E}\}$ be

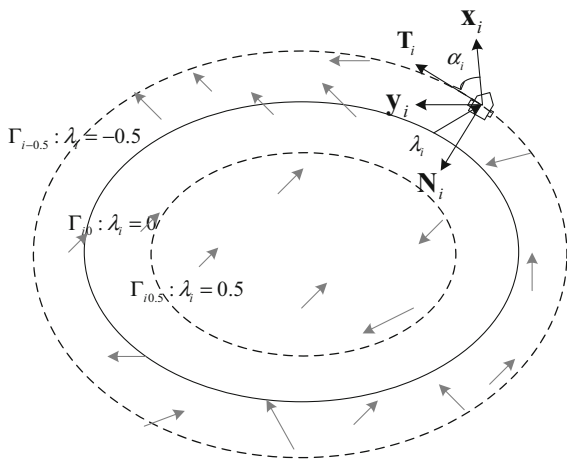


Fig. 3 Path following control design method

the bidirectional graph induced by the inter-uncycle communication topology, where \mathcal{U} denotes the set of n unicycles and \mathcal{E} is a set of data links. Also let \mathcal{N}_i denote the neighbor set of the i th unicycle and we assume that \mathcal{N}_i is time-invariant. Two matrices such as the adjacency matrix $A = [a_{ij}]$ and the Laplacian matrix $L = [l_{ij}]$ are used to represent the graph. The key idea of the formation description on given orbits is based on the consensus design (see Fig. 4), which is widely applied in recent works. Some corresponding explanations can be found in [7, 10–13]. It is said that the formation is maintained when the generalized arc-lengths $\xi_i(t)$ defined in Assumption 1 reach consensus, i.e.,

$$\lim_{t \rightarrow \infty} (\xi_i(t) - \xi_j(t)) = 0. \tag{15}$$

Assumption 1 Each generalized arc-length $\xi_i(s_i(t))$ is a C^2 smooth function of arc-length s_i that $\partial \xi_i / \partial s_i$ satisfies $+\infty > \bar{\epsilon}_M \geq \frac{\partial \xi_i}{\partial s_i} \geq \bar{\epsilon}_m > 0$ and that $\partial^2 \xi_i / \partial s_i^2$ is uniformly bounded.

Remark 3 Let us consider a rigid formation on a set of ellipses as shown in Fig. 4a. Each ellipse is obtained by translating the desired trajectory of the group center along the formation vector $\mathbf{h}_i, i = 1, 2, 3$. Also let \mathbf{z}_i^* denote the starting point associated with Γ_{i0} for computing the arc-length s_i and each pair satisfies $\mathbf{z}_i^* - \mathbf{z}_j^* = \mathbf{h}_i - \mathbf{h}_j$. The rigid formation $\mathbf{z}_i(t) - \mathbf{z}_j(t) = \mathbf{h}_i - \mathbf{h}_j$ is maintained if $s_i(t) = s_j(t)$. To form an in-line formation and move along the concentric orbits with different parameters $a_i \in \mathbb{R}$, it is required that $\xi_i = s_i/a_i$ reach to consensus where the starting point for each orbit is

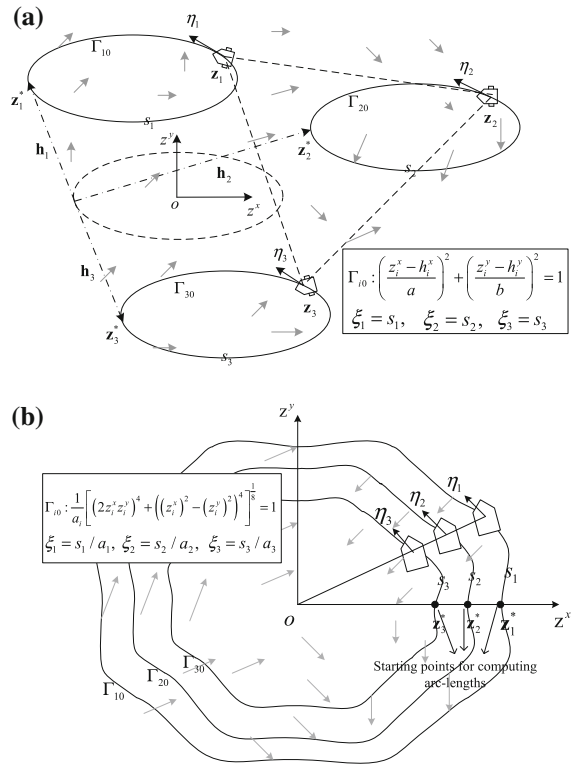


Fig. 4 Formation description on orbits: **a** Rigid formation, **b** In-linear formation

selected as the intersection of the orbit with the horizontal axis (see Fig. 4b).

In some practical situations, multiple unicycles are required for the formation motion at a specified orbital speed. Note that the deviation of the generalized arc-length $\eta_i(t) = d\xi_i(t)/dt$ on the given orbit reflects the orbital speed of the unicycle. This is due to the fact that $\eta_i(t)$ defined in (25) is a product obtained by multiplying the actual linear speed of a unicycle and a parameter with respect to the desired formation pattern. Therefore, $\eta_i(t)$ is regarded as the generalized orbital speed. To accomplish formation motion in accordance with the desired orbital speed, it is required that the generalized orbital speed $\eta_i(t)$ converges to the reference $\eta_*(t)$, i.e.,

$$\lim_{t \rightarrow \infty} \eta_i(t) = \eta_*(t). \tag{16}$$

It must be emphasized that condition $v_i > \|\mathbf{f}\|$ is important to deduce the dynamics of unicycle in the flow field. Differing from the assumption that $v_i > \|\mathbf{f}\|$ in [17–19], we design the controller to ensure it in this

paper. Because of the relationships between v_i and the definition of η_i , here we use

$$\eta_i > \eta^m = 2\bar{\varepsilon}_M f_M \tag{17}$$

to replace $v_i > \|\mathbf{f}\|$. From (16), (25) and Assumption 1, one gets

$$v_{f_i} = \left(\frac{\partial \xi_i}{\partial s_i}\right)^{-1} \eta_i > 2 \left(\frac{\partial \xi_i}{\partial s_i}\right)^{-1} \bar{\varepsilon}_M f_M \geq 2f_M \tag{18}$$

and then

$$\begin{aligned} v_i^2 &= v_{f_i}^2 - 2(\mathbf{f} \cdot \mathbf{x}_i) v_{f_i} + \|\mathbf{f}\|^2 \\ &\geq (v_{f_i} - \|\mathbf{f}\|)^2 > \|\mathbf{f}\|^2. \end{aligned} \tag{19}$$

To move on, we make an assumption as follow:

Assumption 2 The reference $\eta_*(t)$ is uniformly bounded and greater than $2\bar{\varepsilon}_M f_M$. Also $\dot{\eta}_*(t)$ is uniformly bounded.

From the above discussion, we define the coordinated path following control problem in a time-invariant flow field as follows:

Problem 1 Design a coordinated path following controller

$$\begin{aligned} \tau_i &= g_i(\mathbf{z}_i, v_{f_i}, \gamma_i, \omega_i, u_i, \mathbf{f}, \lambda_i, \alpha_i, \mathbf{x}_i, \mathbf{y}_i, s_i, \xi_i, \xi_j, \\ &\quad \eta_*, \dot{\eta}_*) \\ u_i &= \tilde{g}_i(\mathbf{z}_i, v_{f_i}, \gamma_i, \omega_i, \mathbf{f}, \lambda_i, s_i, \xi_i, \eta_i, \xi_j, \eta_j, \eta_*, \dot{\eta}_*) \end{aligned}$$

for the i th unicycle who suffers a time-invariant flow field \mathbf{f} by using its neighbors' communication information such that requirements (12)-(17) are satisfied, where $i \in \mathcal{V}, j \in \mathcal{N}_i$.

Remark 4 The information required in the control consists of two parts. On the one hand, the states $\{\mathbf{z}_i, u_i, v_i, \theta_i, \omega_i, \mathbf{f}\}$ are measured in the inertial reference frame. Then, we use them to calculate the states $\{v_{f_i}, \gamma_i, \mathbf{x}_i, \mathbf{y}_i, d_{\gamma_i}, d_{v_i}, \alpha_i\}$ and the values of $\left\{\lambda_i, \nabla \lambda_i, \nabla^2 \lambda_i, \nabla^3 \lambda_i, s_i, \frac{\partial s_i}{\partial \lambda_i}, \frac{\partial^2 s_i}{\partial \lambda_i^2}, \xi_i, \frac{\partial \xi_i}{\partial s_i}, \frac{\partial^2 \xi_i}{\partial s_i^2}, \eta_i\right\}$ according to the functional forms of $\{\lambda_i, s_i, \xi_i, \eta_i\}$. The definition of each function can be found in Subsects. 2.1 and 3.1. On the other hand, information $\{\xi_i, \eta_i\}$ should be transferred to its neighbors for the cooperation. The details can be found in Subsect. 3.2.

3 Main results

3.1 Coordinated control system

Let $\mathbf{N}_i = -\frac{\nabla \lambda_i}{\|\nabla \lambda_i\|}$ and $\mathbf{T}_i = \begin{bmatrix} 0 & 1 \\ -1 & 0 \end{bmatrix} \mathbf{N}_i$ be the normal vector and the tangent vector to each level orbit, respectively. The direction error α_i between \mathbf{x}_i and \mathbf{T}_i can be defined as

$$\cos \alpha_i = \mathbf{x}_i \cdot \mathbf{T}_i = \mathbf{y}_i \cdot \mathbf{N}_i, \tag{20a}$$

$$\sin \alpha_i = \mathbf{y}_i \cdot \mathbf{T}_i = -\mathbf{x}_i \cdot \mathbf{N}_i. \tag{20b}$$

The time derivative of (20b) yields

$$\begin{aligned} \dot{\alpha}_i &= v_{f_i} \left(\kappa_i^a \cos \alpha_i + \kappa_i^b \sin \alpha_i \right) \\ &\quad - \left(\kappa_{\gamma_i}^u u_i + \kappa_{\gamma_i}^\omega \omega_i + d_{\gamma_i} \right) \end{aligned} \tag{21}$$

where

$$\kappa_i^a = \frac{1}{\|\nabla \lambda_i\|} \mathbf{T}_i \cdot \nabla^2 \lambda_i \mathbf{T}_i,$$

$$\kappa_i^b = -\frac{1}{\|\nabla \lambda_i\|} \mathbf{T}_i \cdot \nabla^2 \lambda_i \mathbf{N}_i$$

and $\nabla^2 \lambda_i$ is the Hessian matrix of $\lambda_i(\mathbf{z}_{f_i})$. Since the orbit value with respect to Γ_{i0} is 0, the position error of path following can be represented as $\lambda_i(\mathbf{z}_{f_i})$, and then, the dynamics of position error of path following can be written as

$$\dot{\lambda}_i = \nabla \lambda_i \cdot \dot{\mathbf{z}}_i = v_{f_i} \|\nabla \lambda_i\| \sin \alpha_i. \tag{22}$$

Since the movement of the i th unicycle projected to \mathbf{T}_i leads to the variation in arc-length s_i while the motion along the direction of concentric compression causes the orbit change which also induces the changes of the arc-length, the arc-length s_i measured from the starting point can be written as

$$s_i(\lambda_i, \phi_i) \triangleq \int_{\phi_i^*}^{\phi_i} \frac{\partial s_i(\lambda_i, \tau)}{\partial \tau} d\tau. \tag{23}$$

where the starting points for computing s_i around each level orbit in Ω_i are chosen based on the same value of arc-length parameter ϕ_i^* corresponding to the starting point selected on the given orbit Γ_{i0} . When the unicycle moves, the variation of generalized arc-length is

$$\begin{aligned} \dot{\xi}_i &= \frac{\partial \xi_i}{\partial s_i} \left(\frac{\partial s_i}{\partial \phi_i} \dot{\phi}_i + \frac{\partial s_i}{\partial \lambda_i} \dot{\lambda}_i \right) \\ &= \frac{\partial \xi_i}{\partial s_i} \left(\frac{ds_i}{dt} \Big|_{\lambda_i=const} + \frac{\partial s_i}{\partial \lambda_i} \|\nabla \lambda_i\| v_{f_i} \sin \alpha_i \right) \\ &= \frac{\partial \xi_i}{\partial s_i} v_{f_i} \left(\cos \alpha_i + \frac{\partial s_i}{\partial \lambda_i} \|\nabla \lambda_i\| \sin \alpha_i \right). \end{aligned} \tag{24}$$

In the next subsection, each unicycle is driven to arrive at its given orbit, which implies $\alpha_i(t) = 0$ and then $\dot{\xi}_i(t) = \frac{\partial \xi_i}{\partial s_i} v_{f_i}$. In order to reduce the amount of calculation and simplify the design of the control laws, η_i is defined as

$$\eta_i = \frac{\partial \xi_i}{\partial s_i} v_{f_i}. \tag{25}$$

Then, the variation of the generalized arc-length can be written as

$$\dot{\xi}_i = \eta_i + d_{\eta_i} \tag{26}$$

where $d_{\eta_i} = \eta_i \left(-2 \sin^2 \frac{\alpha_i}{2} + \frac{\partial s_i}{\partial \lambda_i} \|\nabla \lambda_i\| \sin \alpha_i \right)$. Differentiating η_i , we have

$$\begin{aligned} \dot{\eta}_i &= \frac{\partial \xi_i}{\partial s_i} \left(\kappa_{v_{f_i}}^u u_i + \kappa_{v_{f_i}}^\omega \omega_i + d_{v_{f_i}} \right) \\ &\quad + \frac{\partial^2 \xi_i}{\partial s_i^2} v_{f_i} (\eta_i + d_{\eta_i}). \end{aligned} \tag{27}$$

3.2 Backstepping design

Step 1. Convergence of $\lambda_i, \alpha_i, \xi_i - \xi_j, \eta_i - \eta_*$: The control Lyapunov function is selected as follows:

$$\begin{aligned} V_I &= \sum_{i=1}^n h_i(\lambda_i) - \sum_{i=1}^n \ln \left(\cos^2 \frac{\alpha_i}{2} \right) \\ &\quad + \frac{k_0}{4} \sum_{i=1}^n \sum_{j=1}^n a_{ij} (\xi_i - \xi_j)^2 \\ &\quad + \sum_{i=1}^n \left(\ln \left(\frac{\eta_i - \eta^m}{\eta_* - \eta^m} \right) + \frac{\eta_* - \eta^m}{\eta_i - \eta^m} - 1 \right) \end{aligned} \tag{28}$$

where $k_0 > 0$ and $h_i(\lambda_i)$ is a C^2 smooth, nonnegative function on $(-\varepsilon_i, \varepsilon_i)$. Let $h_i(\lambda_i)$ and $\nabla h_i = dh_i/d\lambda_i$ satisfy the following conditions:

- (C1) $h_i(\lambda_i) \rightarrow +\infty$ and $\nabla h_i \rightarrow -\infty$ as $\lambda_i \rightarrow -\varepsilon_i$.
- (C2) $h_i(\lambda_i) \rightarrow +\infty$ and $\nabla h_i \rightarrow +\infty$ as $\lambda_i \rightarrow \varepsilon_i$.
- (C3) $h_i(\lambda_i) = 0$ if and only if $\lambda_i = 0$.

There are many functions that satisfy all the above properties of $h_i(f_i)$. An example is

$$\begin{aligned} h_i(f_i) &= \int_{f_i^*}^{f_i} \left[c_1 \left(\frac{1}{\varepsilon_i - \tau} - \frac{1}{\varepsilon_i + \tau} \right) \right. \\ &\quad \left. + c_2 (\ln(\varepsilon_i + \tau) - \ln(\varepsilon_i - \tau)) \right] d\tau, \end{aligned}$$

where $f_i^* = f_i(\mathbf{z}_i(0)) \in \Omega_i$ and $c_1, c_2 > 0$.

In the function (28), the first term contributes to forcing the trajectory of each unicycle to its given orbit and

stays in Ω_i when it start from Ω_i . It vanishes when $\lambda_i = 0$. The second term aligns the direction of each unicycle's motion and the tangent vector to the orbit. It vanishes when $\alpha_i = 0$. The next term ensures the consensus of the generalized arc-lengths. It vanishes when $\xi_i = \xi_j$. The fourth term guarantees that η_i converge to the reference and $v_i > \|\mathbf{f}\|$ for all time. It vanishes when $\eta_i = \eta_*$.

The time derivation of V_I is

$$\begin{aligned} \dot{V}_I &= \sum_{i=1}^n \tan \frac{\alpha_i}{2} \left(\Delta \alpha_i - \left(\kappa_{\gamma_i}^u u_i + \kappa_{\gamma_i}^\omega \omega_i + d_{\gamma_i} \right) \right) \\ &\quad + \sum_{i=1}^n (\eta_i - \eta_*) \left((\eta_i - \eta^m)^{-2} \frac{\partial \xi_i}{\partial s_i} \right. \\ &\quad \left. \times \left(\kappa_{v_{f_i}}^u u_i + \kappa_{v_{f_i}}^\omega \omega_i + d_{v_{f_i}} \right) + \Delta \eta_i \right) \end{aligned} \tag{29}$$

where

$$\begin{aligned} \Delta \alpha_i &= v_{f_i} \left(\kappa_i^a \cos \alpha_i + \kappa_i^b \sin \alpha_i \right) \\ &\quad + 2v_{f_i} \nabla h_i \|\nabla \lambda_i\| \cos^2 \frac{\alpha_i}{2} \\ &\quad + k_0 \eta_i \left(-\sin \alpha_i + 2 \frac{\partial s_i}{\partial \lambda_i} \|\nabla \lambda_i\| \cos^2 \frac{\alpha_i}{2} \right) \\ &\quad \times \sum_{j=1}^n a_{ij} (\xi_i - \xi_j), \\ \Delta \eta_i &= (\eta_* - \eta^m)^{-2} \frac{\partial^2 \xi_i}{\partial s_i^2} v_{f_i} (\eta_i + d_{\eta_i}) \\ &\quad + k_0 \sum_{j=1}^n a_{ij} (\xi_i - \xi_j) - (\eta_i - \eta^m)^{-1} (\eta_* - \eta^m)^{-1} \dot{\eta}_*. \end{aligned}$$

Here, we first use the unicycle's angular velocity ω_i as the virtual control $\bar{\omega}_i$ and the acceleration input u_i to fulfill the coordinated path following control problem.

The choices are

$$\begin{bmatrix} \kappa_{\gamma_i}^u & \kappa_{\gamma_i}^\omega \\ \kappa_{v_{f_i}}^u & \kappa_{v_{f_i}}^\omega \end{bmatrix} \begin{bmatrix} u_i \\ \bar{\omega}_i \end{bmatrix} = \begin{bmatrix} g_{\alpha_i} \\ g_{\eta_i} \end{bmatrix} \tag{30}$$

where

$$\begin{aligned} g_{\alpha_i} &= \Delta \alpha_i + k_1 \sin \frac{\alpha_i}{2} - d_{\gamma_i}, \\ g_{\eta_i} &= -(\eta_i - \eta^m)^2 \left(\frac{\partial \xi_i}{\partial s_i} \right)^{-1} \\ &\quad \times \left(\Delta \eta_i + k_2 (\eta_i - \eta_*) + k_3 \sum_{j=1}^n a_{ij} (\eta_i - \eta_j) \right) - d_{v_{f_i}}. \end{aligned}$$

Obviously, Eq. (30) has a unique solution

$$u_i = g_{\kappa_i}^{-1} \left(\kappa_{\gamma_i}^u g_{\alpha_i} - \kappa_{\nu_{fi}}^u g_{\eta_i} \right), \tag{31}$$

$$\bar{\omega}_i = g_{\kappa_i}^{-1} \left(\kappa_{\nu_{fi}}^\omega g_{\alpha_i} - \kappa_{\gamma_i}^\omega g_{\eta_i} \right). \tag{32}$$

Remark 5 Since the speed of particle in [17–19] is fixed (that is, unit-speed), the authors just assume that the flow field satisfies $\|\mathbf{f}\| < 1$. In this paper, the speed is controllable and serves two targets. On the one hand, the linear acceleration contributes to accomplishing the temporal and spatial formation motions along given orbits. On the other hand, the goal such that the speed is greater than $\|\mathbf{f}\|$ and converges to the reference is guaranteed by using the speed control. For the latter object, a potential function used in collision avoidance [21] is introduced in this paper, which can be found in the last term in (28).

Remark 6 In the flow field, the virtual control $\bar{\omega}_i$ and the acceleration input u_i work together to achieve path following and formation motion, while they are separately responsible for path following and formation motion in [11]. All these changes are due to the effect of the external flow field.

Now, substituting (31) and (32) into (29) results in

$$\begin{aligned} \dot{V}_I &= -k_1 \sum_{i=1}^n \frac{\sin^2 \frac{\alpha_i}{2}}{\cos \frac{\alpha_i}{2}} - k_2 \sum_{i=1}^n (\eta_i - \eta_*)^2 \\ &\quad - k_3 (\eta - \eta_* \mathbf{1}_n)^T L (\eta - \eta_* \mathbf{1}_n) \leq 0 \end{aligned} \tag{33}$$

where $\eta = [\eta_1, \dots, \eta_n]^T$ and $\mathbf{1}_n = [1, \dots, 1]^T$.

To accomplish the control input τ_i , the error variable is introduced such as

$$\omega_{e_i} = \omega_i - \bar{\omega}_i \tag{34}$$

which should be driven to zero, and re-write \dot{V}_I as

$$\begin{aligned} \dot{V}_I &= -k_1 \sum_{i=1}^n \frac{\sin^2 \frac{\alpha_i}{2}}{\cos \frac{\alpha_i}{2}} - k_2 \sum_{i=1}^n (\eta_i - \eta_*)^2 \\ &\quad - k_3 (\eta - \eta_* \mathbf{1}_n)^T L (\eta - \eta_* \mathbf{1}_n) + \sum_{i=1}^n \omega_{e_i} \Delta_{e_i} \end{aligned} \tag{35}$$

where

$$\Delta_{e_i} = -\kappa_{\gamma_i}^\omega \tan \frac{\alpha_i}{2} + \kappa_{\nu_{fi}}^\omega \frac{\partial \xi_i}{\partial s_i} (\eta_i - \eta^m)^{-2} (\eta_i - \eta_*).$$

Step 2. Backstepping for ω_{e_i} : The second control Lyapunov function is given by

$$V_{II} = V_I + \sum_{i=1}^n \omega_{e_i}^2. \tag{36}$$

Taking the time derivative of both sides of Eq. (36) along the solution of (31), one gets

$$\begin{aligned} \dot{V}_{II} &= -k_1 \sum_{i=1}^n \frac{\sin^2 \frac{\alpha_i}{2}}{\cos \frac{\alpha_i}{2}} - k_2 \sum_{i=1}^n (\eta_i - \eta_*)^2 \\ &\quad - k_3 (\eta - \eta_* \mathbf{1}_n)^T L (\eta - \eta_* \mathbf{1}_n) \\ &\quad + \sum_{i=1}^n \omega_{e_i} (\tau_i - \dot{\bar{\omega}}_i - \Delta_{e_i}). \end{aligned} \tag{37}$$

We design the yaw force τ_i as follows:

$$\tau_i = \dot{\bar{\omega}}_i + \Delta_{e_i} - k_4 \omega_{e_i} \tag{38}$$

where $k_4 > 0$, which yields

$$\begin{aligned} \dot{V}_{II} &= -k_1 \sum_{i=1}^n \frac{\sin^2 \frac{\alpha_i}{2}}{\cos \frac{\alpha_i}{2}} - k_2 \sum_{i=1}^n (\eta_i - \eta_*)^2 \\ &\quad - k_3 (\eta - \eta_* \mathbf{1}_n)^T L (\eta - \eta_* \mathbf{1}_n) \\ &\quad - k_4 \sum_{i=1}^n \omega_{e_i}^2 \leq 0. \end{aligned} \tag{39}$$

3.3 Stability analysis

Under the control laws (31) and (38), the equation of the closed-loop system for λ_i is denoted as (22), the equation of the closed-loop system for α_i is (21) where $\dot{\omega}_i$ satisfies (32), and the equation of the closed-loop system for the relative generalized arc-length is

$$\dot{\xi}_i - \dot{\xi}_j = \eta_i + d_{\eta_i} - \eta_j - d_{\eta_j}, \tag{40}$$

the equation of the closed-loop system for $\eta_i - \eta_*$ satisfies

$$\begin{aligned} \dot{\eta}_i - \dot{\eta}_* &= \left(\frac{\eta_i - \eta^m}{\eta_* - \eta^m} - 1 \right) \dot{\eta}_* - (\eta_i - \eta^m)^2 \\ &\quad \times \left(k_0 \sum_{j=1}^n a_{ij} (\xi_i - \xi_j) + k_2 (\eta_i - \eta_*) \right. \\ &\quad \left. + k_3 \sum_{j=1}^n a_{ij} (\eta_i - \eta_j) \right). \end{aligned} \tag{41}$$

Theorem 1 Consider a family of level closed curves of the orbit function constructed by concentric compression. Suppose the generalized arc-lengths and the

reference $\eta_*(t)$ satisfy Assumption 1 and Assumption 2, respectively. Assume the initial conditions of unicycles make the initial value of V_{II} given in (36) finite. Then, Problem 1 is solved via the linear acceleration force (31) and the angular acceleration force (38) if the communication topology is connected.

Proof The set $\Phi = \{(\lambda_i, \alpha_i, \xi_i - \xi_j, \eta_i - \eta_*, \omega_{e_i}) \mid V_{II} \leq c\}$ such that $V_{II} \leq c$, for $c > 0$, is closed by continuity. Since $|\lambda_i| < \varepsilon_i$ due to the boundedness of V_{II} , α_i is defined in $(-\pi, \pi]$, $|\xi_i - \xi_j| \leq \sqrt{4c}$, and $|\eta_i| \leq h_{\eta_i}^{-1}(c) + \eta_* + \eta^m$ where $h_{\eta_i} = \ln((\eta_i - \eta^m) / (\eta_* - \eta^m)) + (\eta_i - \eta^m) / (\eta_* - \eta^m) - 1$, the set Φ is compact. On the compact set Φ , $|\partial s_i(\lambda_i, \phi_i) / \partial \lambda_i|$ and $|\partial^2 s_i(\lambda_i, \phi_i) / \partial \lambda_i^2|$ are bounded because $\phi_i \in [0, 2\pi)$. $\|\nabla \lambda_i\|$ is bounded by continuity. Since $\partial \xi_i / \partial s_i$ is bounded away from 0, $v_{f_i} = (\frac{\partial \xi_i}{\partial s_i})^{-1} \eta_i$ is also bounded on Φ . Thus, the closed-loop system is Lipschitz continuous on the set Φ and a solution exists and is unique.

Because the value of V_{II} is time independent and non-increasing, we conclude that the entire solution stays in Φ and then $\eta_i > \eta^m$ when the initial value of V_{II} is finite. At the same time, $|\lambda_i(\mathbf{z}_i(t))| < \varepsilon_i$ is satisfied by (C1) and (C2). Applying the invariance-like theorem, it follows that the trajectories of the closed-loop system will converge to the set inside the region $E = \{(\lambda_i, \alpha_i, \xi_i - \xi_j, \eta_i - \eta_*, \omega_{e_i}) \mid \dot{V}_{II} = 0\}$ as $t \rightarrow \infty$, that is

$$\alpha_i = 0, \eta_i = \eta_*, \omega_{e_i} = 0, \tag{42a}$$

$$(\eta - \eta_* \mathbf{1}_n)^T L (\eta - \eta_* \mathbf{1}_n) = 0 \Rightarrow \eta_i = \eta_j. \tag{42b}$$

On the set E , the equations of the whole closed-loop system become

$$\dot{\lambda}_i = 0, \tag{43a}$$

$$\begin{aligned} \dot{\alpha}_i &= -2v_{f_i} \nabla h_i \|\nabla \lambda_i\| \\ &\quad - 2k_0 \eta_i \frac{\partial s_i}{\partial \lambda_i} \|\nabla \lambda_i\| \sum_{j=1}^n a_{ij} (\xi_i - \xi_j), \end{aligned} \tag{43b}$$

$$\dot{\xi}_i - \dot{\xi}_j = 0, \tag{43c}$$

$$\dot{\eta}_i - \dot{\eta}_* = -k_0 (\eta_i - \eta^m)^2 \sum_{j=1}^n a_{ij} (\xi_i - \xi_j). \tag{43d}$$

In the following, we will show $\xi_i - \xi_j \rightarrow 0$ as $t \rightarrow \infty$. On the set E , from (43c) one gets that $\xi_i - \xi_j$ is constant. Applying the extension of the Barbalat lemma in [22], from (43d) and Assumption 2,

$\dot{\eta}_i - \dot{\eta}_* = -k_0 (\eta_i - \eta^m)^2 \sum_{j=1}^n a_{ij} (\xi_i - \xi_j) \rightarrow 0$. Since $\eta_i - \eta^m \rightarrow \eta_* - \eta^m \neq 0$ as $t \rightarrow \infty$, one gets $L\xi = 0$ where $\xi = [\xi_1, \dots, \xi_n]^T$, which implies that $\xi_i - \xi_j \rightarrow 0$ as $t \rightarrow \infty$ when the communication topology is connected.

Because $\xi_i - \xi_j \rightarrow 0$ as $t \rightarrow \infty$, the equation of the closed-loop system for α_i on the set E is changed to

$$\dot{\alpha}_i = -2v_{f_i} \nabla h_i \|\nabla \lambda_i\|. \tag{44}$$

It is easy to check that $\lim_{t \rightarrow \infty} v_{f_i} = (\partial \xi / \partial s_i) \eta_* > 0$ is uniformly continuous and bounded from Assumption 1 and 2. The details can be found in [11]. From (43a), λ_i approaches to a constant and thus ∇h_i approaches to a constant. Therefore, $-2\nabla h_i v_{f_i} \|\nabla \lambda_i\|$ is uniformly continuous. Applying the extension of the Barbalat lemma [22], from (44) we have $\dot{\alpha}_i \rightarrow 0$ as $t \rightarrow \infty$. Because $\lim_{t \rightarrow \infty} v_{f_i} \|\nabla \lambda_i\| \neq 0$, one gets $\nabla h_i \rightarrow 0$ as $t \rightarrow \infty$. By (C3), λ_i approaches to 0. \square

4 Simulation results

In this section, the proposed control law is applied to coordinate four unicycles moving along the given closed curves. The communication topology is shown in Fig. 5. The control gains are selected as $k_0 = 20, k_j = 10, j = 1, \dots, 5$. The non-uniform flow field is $\mathbf{f}_i = [-0.25 * \sin(2 * \pi * 5/360 * (z_i^x + z_i^y)), 0.25 * \cos(2 * \pi * 5/360 * (z_i^x + z_i^y))]^T$.

Case 1 The given orbits are a set of concentric ellipses with different semi-major axis and semi-minor axis, that is

$$\left(\frac{z_i^x}{3l_i}\right)^2 + \left(\frac{z_i^y}{2l_i}\right)^2 = 1$$

where $l_i = 1 + 0.5(i - 1), i = 1, \dots, 4$. In this case, four unicycles are required to form the in-line formation with $\eta_*(t) = 2 + 0.2 \sin(t)$. The starting points are

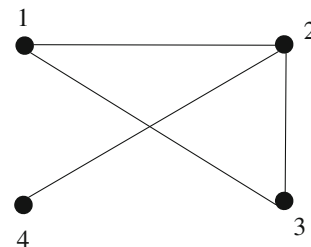


Fig. 5 Communication topology

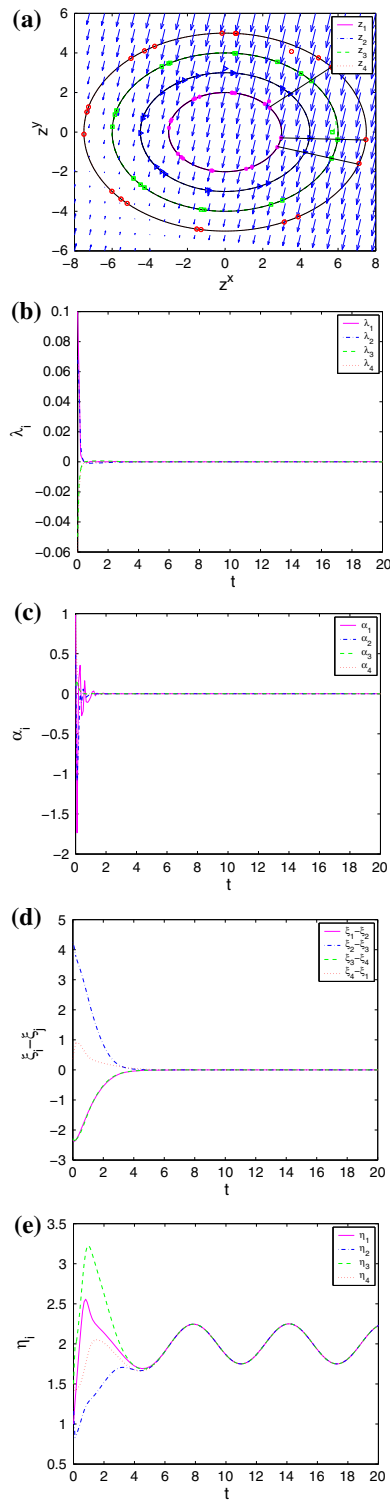


Fig. 6 In-linear formation motion along convex orbits: **a** Plot of movements, **b** Plot of λ_i , **c** Plot of α_i , **d** Plot of $\xi_i - \xi_j$, **e** Plot of η_i

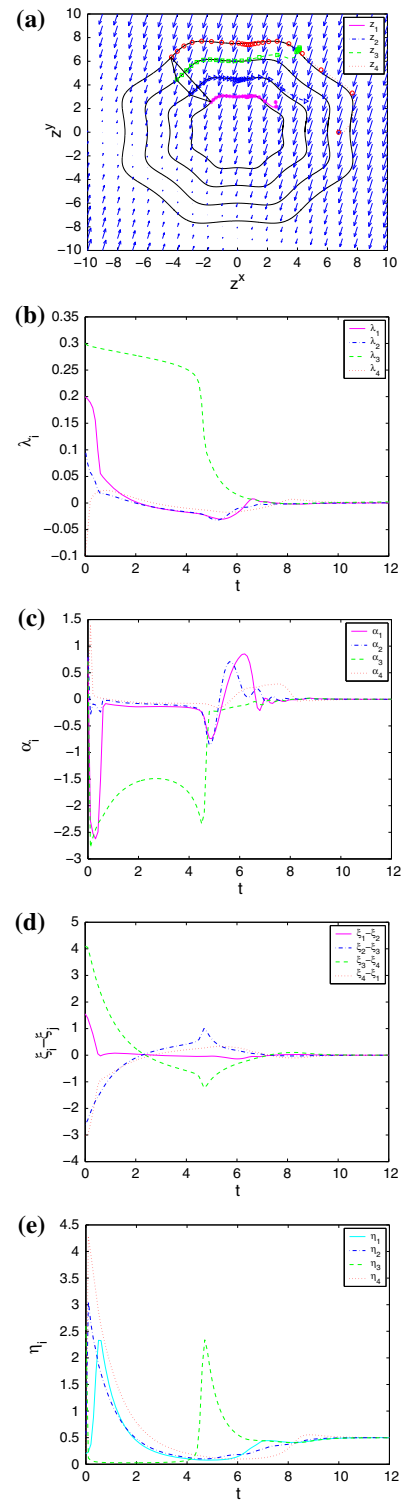


Fig. 7 Trapezoidal formation motion along non-convex orbits: **a** Plot of movements, **b** Plot of λ_i , **c** Plot of α_i , **d** Plot of $\xi_i - \xi_j$, **e** Plot of η_i

defined as the intersection of the orbits with the positive horizontal axis of \mathcal{W} , and we choose the general arc-lengths as $\xi_j = s_i/l_i$. The movement of unicycles is shown in Fig. 6a. From this figure, we can see that four unicycles finally move along the set of given orbits and form the desired formation. The path following errors f_i and α_i tend to zero and are plotted in Fig. 6b, c, respectively. Figure 6d demonstrates that ξ_i reaches consensus and Fig. 6e shows η_i converges to the reference. According to these pictures, we conclude that our control law is suitable to deal with formation motion around convex curves.

Case 2 The given orbits are a set of concentric super-ellipses (non-convex orbits) such as

$$\frac{1}{a_i} \left[(2z_i^x z_i^y)^4 + \left((z_i^x)^2 - (z_i^y)^2 \right)^4 \right]^{\frac{1}{8}} = 1$$

where $a_i = 3 + 0.5(i - 1)$, $i = 1, \dots, 4$. In this case, the desired pattern is that forming a trapezoidal formation with $\eta_* = 0.5$. The starting points are defined as the intersection of the orbits with the positive horizontal axis of \mathcal{W} , and we choose $\xi_j = s_j/a_j$; ($j = 1, 4$), $\xi_2 = s_2/a_2 + \pi/6$ and $\xi_3 = s_3/a_3 + \pi/8$. The movement of unicycles is shown in Fig. 7a. From this figure, we can see that four unicycles finally move along the set of given orbits and form the desired formation. The path following errors f_i and α_i tend to zero and are plotted in Fig. 7b, c, respectively. Figure 7d demonstrates that ξ_i reaches consensus, and Fig. 7e shows η_i converges to the reference. According to these pictures, coordinated non-convex curve path following control problem is also solved via our proposed controller.

5 Conclusion

In this paper, our previous geometric extension design [11] is developed to deal with coordinated path following control of unicycles in an external time-invariant flow field. Both temporal and spatial formations is achieved by introducing the acceleration control. The potential function is used to force each unicycle's speed greater than the magnitude of flow. The validity of the proposed approach is confirmed by theoretical analysis and numerical simulation.

Acknowledgments This work was supported in part by the National Natural Science Foundation of China under Grants

61203356, 61273110, 61374069, 61473081, in part by Doctoral Fund of Ministry of Education of China under Grant 20110092120025, in part by the open fund of Key Laboratory of Measurement and Control of Complex Systems of Engineering, Ministry of Education under Grant MCCSE2014B01, and in part by a Project Funded by the Priority Academic Program Development of Jiangsu Higher Education Institutions.

References

- Chong, C., Kumar, S.P.: Sensor networks: evolution, opportunities, and challenges. *Proc. IEEE* **91**(8), 1247–1256 (2003)
- Leonard, N.E., Paley, D.A., Lekien, F., Sepulchre, R.D., Frantantoni, M., Davis, R.E.: Collective motion, sensor networks, and ocean sampling. *Proc. IEEE* **95**(1), 48–74 (2007)
- MBARI, Autonomous ocean sampling network, <http://www.mbari.org/aosn/NontereyBay2003/>
- Princeton University, Adaptive Sampling and Prediction, <http://www.princeton.edu/dcs/ls/asap/>
- Sepulchre, R., Paley, D.A., Leonard, N.E.: Stabilization of planar collective motion: all-to-all communication. *IEEE Trans. Autom. Control* **52**(5), 811–824 (2007)
- Sepulchre, R., Leonard, N.E., Paley, D.A.: Stabilization of symmetric formations to motion around convex loops. *Syst. Contr. Lett.* **57**(3), 209–215 (2008)
- Ghabcheloo, R., Pascoal, A., Silvestre, C., Kaminer, I.: Coordinated path following control of multiple wheeled robots with directed communication links. In: *IEEE Conference on Decision and Control, and the European Control Conference*, Seville, Spain, pp. 7084–7089 (2005)
- Ghabcheloo, R., Pascoal, A., Silvestre, C., Kaminer, I.: Nonlinear coordinated path following control of multiple wheeled robots with bidirectional communication constraints. *Int. J. Adapt. Control Signal Process.* **21**(2–3), 133–137 (2007)
- Zhang, F., Leonard, N.E.: Coordinated patterns of unit speed particles on a closed curve. *Syst. Contr. Lett.* **56**(6), 397–407 (2007)
- Zhang, F., Fratantoni, D.M., Paley, D.A., Lund, J., Leonard, N.E.: Control of coordinated patterns for ocean sampling. *Int. J. Control* **80**(7), 1186–1199 (2007)
- Chen, Y.-Y., Tian, Y.-P.: A curve extension design for coordinated path following control of unicycles along given convex loops. *Int. J. Control* **84**(10), 1729–1745 (2011)
- Chen, Y.-Y., Tian, Y.-P.: Coordinated adaptive control for 3D formation tracking with a time-varying orbital velocity. *IET Control Theory Appl.* **7**(5), 646–662 (2013)
- Chen, Y.-Y., Tian, Y.-P.: Formation tracking and attitude synchronization control of underactuated ships along closed orbits. *International journal of Robust and Nonlinear Control*, Published online: doi:10.1002/rnc.3246 (2014)
- Das, A., Lewis, F.L.: Cooperative adaptive control for synchronization of second-order system with unknown nonlinearities. *Int. J. Robust Nonlinear Control* **21**(13), 1509C–1524C (2011)
- Hu, G.Q.: Robust consensus tracking of a class of second-order multi-agent dynamic systems. *Syst. Control Lett.* **61**(1), 134C–142C (2012)

16. Peng, Z.H., Wang, D., Li, T., Wu, Z.L.: Leaderless and leader-follower cooperative control of multiple marine surface vehicles with unknown dynamics. *Nonlinear Dyn.* **74**(1–2), 95–106 (2013)
17. Paley, D.A., Petersion, C.: Stabilization of collective motion in a time-invariant flow field. *AIAA J. Guid. Control Dyn.* **32**(3), 771–779 (2009)
18. Mellish, R., Napora, S., Paley, D.A.: Backstepping control design for motion coordination of self-propelled vehicles in a flowfield. *Int. J. Robust Nonlinear Control* **21**(12), 1452–1466 (2011)
19. Paley, D.A., Techy, L., Woolsey, C.A.: Coordinated perimeter patrol with minimum-time alert response. In: *AIAA J. Guidance, Navigation, and Control Conference and Exhibit*, Chicago, IL, United states, pp. 2009–6210 (2009)
20. Weisstein, E.W.: Superellipse, <http://mathworld.wolfram.com/Superellipse.html>
21. Chen, Y.-Y., Tian, Y.-P.: A backstepping design for directed formation control of three-coleader agents in the plane. *Int. J. Robust Nonlinear Control* **9**(7), 729–745 (2009)
22. Micaelli, A., Samson, C.: Trajectory tracking for unicycle-type and two-steering-wheels mobile robots. INRIA report 2097, (1993)